




Article

# Modeling the Solvent Extraction of Cadmium(II) from Aqueous Chloride Solutions by 2-pyridyl Ketoximes: A Coordination Chemistry Approach

Eleni C. Mazarakioti <sup>1</sup>, Amaia Soto Beobide <sup>2</sup>, Varvara Angelidou <sup>1</sup>,  
Constantinos G. Efthymiou <sup>1</sup>, Aris Terzis <sup>3</sup>, Vassilis Psycharis <sup>3,\*</sup>, George A. Voyiatzis <sup>2,\*</sup> and  
Spyros P. Perlepes <sup>1,2,\*</sup>

<sup>1</sup> Department of Chemistry, University of Patras, 265 04 Patras, Greece; eleni.mazarakioti@uv.es (E.C.M.); varvara\_angelidou@hotmail.com (V.A.); dinosef@yahoo.com (C.G.E.)

<sup>2</sup> Foundation for Research and Technology-Hellas (FORTH), Institute of Chemical Engineering Sciences (ICE-HT), Platani, P.O. Box 1414, 265 04 Patras, Greece; asoto@iceht.forth.gr

<sup>3</sup> Institute of Nanoscience and Nanotechnology, NCSR "Demokritos", 153 10 Aghia Paraskevi Attikis, Greece; a.terzis@inn.demokritos.gr

\* Correspondence: v.psycharis@inn.demokritos.gr (V.P.); gvog@iceht.forth.gr (G.A.V.); perlepes@patreas.upatras.gr (S.P.P.); Tel.: +30-210-6503346 (V.P.); +30-2610-965253 (G.A.V.); +30-2610-996730 (S.P.P.)

Academic Editor: Carl J. Carrano

Received: 13 May 2019; Accepted: 11 June 2019; Published: 13 June 2019



**Abstract:** The goal of this work is to model the nature of the chemical species  $[\text{CdCl}_2(\text{extractant})_2]$  that are formed during the solvent (or liquid-liquid) extraction of the toxic cadmium(II) from chloride-containing aqueous media using hydrophobic 2-pyridyl ketoximes as extractants. Our coordination chemistry approach involves the study of the reactions between cadmium(II) chloride dihydrate and phenyl 2-pyridyl ketoxime (phpaoH) in water-containing acetone. The reactions have provided access to complexes  $[\text{CdCl}_2(\text{phpaoH})_2] \cdot \text{H}_2\text{O}$  ( $1 \cdot \text{H}_2\text{O}$ ) and  $\{[\text{CdCl}_2(\text{phpaoH})]\}_n$  ( $2$ ); the solid-state structures of which have been determined by single-crystal X-ray crystallography. In both complexes, phpaoH behaves as an  $N,N'$ -bidentate chelating ligand. The complexes have been characterized by solid-state IR and Raman spectra, and by solution  $^1\text{H}$  NMR spectra. The preparation and characterization of  $1 \cdot \text{H}_2\text{O}$  provide strong evidence for the existence of the species  $[\text{CdCl}_2(\text{extractant})_2]$  that have been proposed to be formed during the liquid-liquid extraction process of Cd(II), allowing the efficient transfer of the toxic metal ion from the aqueous phase into the organic phase.

**Keywords:** cadmium(II); coordination chemistry; model studies for liquid-liquid extraction; phenyl 2-pyridyl ketoxime as ligand; 2-pyridyl ketoximes as cadmium(II) extractants; Raman spectra; single-crystal X-ray structures

## 1. Introduction

The rapid industrialization of our society during the 20th century provided humans with a better quality of life, but it has simultaneously generated a series of environmental issues; one serious problem is associated with the accumulation of heavy toxic metal ions in industrial effluents [1]. Cadmium(II) is a very toxic metal ion, being introduced into the environment by anthropogenic activities, such as the production of alkaline batteries, lead-zinc mining, photography, electroplate, and pigments [2], thus affecting plants and humans. Exposure of humans to elevated Cd(II) concentrations causes several acute and chronic harmful symptoms in the liver, kidneys, and cardiovascular and nervous systems [1]. Diseases caused by Cd(II) toxicity are proteinuria, aminoaciduria, cadmium-promoted creatinuria,

cadmium-induced renal tubular dysfunction, and a form of itai-itai, the latter arising from drinking water contaminated with this metal ion and leading to osteomalacia and bone decalcification [3]. These macroscopic symptoms require the presence of soluble forms of Cd(II), which are mobilizable into waters, the food chain, and into the cellular fluids of organisms [4]. The toxicity of this metal ion is mainly attributed to its strong interactions with the cysteinyl sulfur atoms of enzymes and proteins [5]. Due to the non-biodegradable and non-decomposable nature of Cd(II), efficient methods for its removal from wastewater should be developed. Several methods for this use have been designed and developed, such as ion exchange, chemical precipitation, membrane separation, adsorption methods, and solvent extraction [1,6,7]. This work is related to the latter method.

Solvent extraction is increasingly used for both the recovery of useful metals and the removal of toxic metal ions. In a typical flow sheet of the former process [8], the metal contents in an ore are leached into an aqueous solution, and the valuable metal ion is then transferred to a water-immiscible solvent where the unit operations of concentration and separation take place. Stripping back to provide a pure electrolyte allows the recovery of the metal by electroreduction. The removal of toxic metal ions using solvent extraction occurs through the complexation of the metal ion with an organic ligand to form a species that is transferred from the aqueous to the organic phase in a two-phase system [9]. Hexane and kerosene are mainly used in industry due to their low toxicity, but most laboratory studies have been carried out with chloroform as the organic phase. Carbon dioxide is also used for the solid-liquid extraction of heavy metal ions from contaminated soils. There are three types of *liquid-liquid* extraction: (a) The case where the extractant, i.e., the organic ligand, and the metal ion source are both soluble in the aqueous phase, and the extracted complex is soluble in the organic phase; (b) the case where both the extractant and the metal ion source are insoluble in the aqueous phase and the complexation takes place at the interphase surface, and the metal species is then transferred into the organic phase; (c) the case where the extractant is soluble only in the organic phase and the metal ion source is soluble only in the aqueous phase, the complexation reaction occurring again at the interphase surface before the transfer of the metal ion-extractant complex into the organic phase.

Most efficient extractants are chelating or macrocyclic ligands; the reason for this is the high thermodynamic stability of the resulting metal complexes due to the chelate or macrocyclic effects [10]. After decades of research, it is now well established that the main requirements for an effective extractant are the following: (i) Fast binding of the toxic metal ion by the extractant; (ii) good stability of the metal ion-extractant complex against hydrolysis; (iii) selective metal ion complexation with no or weak affinity for group 1 (alkali ions) and 2 (alkaline earth ions) metal ions, which are present at high concentrations in natural and waste waters; (iv) high enough binding strength for the metal ion to be extracted; (v) reversible complexation reaction, which allows for the complete recovery of the metal ion without significant extractant decomposition or destruction.

Several extractants have been used for the liquid-liquid extraction of toxic Cd(II), including [9,11,12] organophosphorus derivatives, dithiocarbamates, xanthates, EDTA derivatives, crown ethers, azacrowns, derivatized calix[4]arenes, substituted 8-quinolols, pyridine carboxamides, and *pyridyl ketoximes*. In an excellent study, which has been the stimulus of the present work, Parus and co-workers investigated the solvent extraction of Cd(II) from aqueous chloride solutions using 1-(2-pyridyl)-trideca-1-one oxime (2PC12) and 1-(2-pyridyl)-pentadecane-1-one oxime (2PC14) [12]. The structural formulae of the extractants are presented in Figure 1. The influence of the extractant, metal ion and chloride ion concentration, and the nature of various polar and non-polar solvents (diluent) on the extraction efficiency was studied in detail. Cadmium(II) was effectively extracted using chloroform (CHCl<sub>3</sub>) or hydrocarbons mixed with decan-1-ol as organic phases, and stripped from the loaded organic phase with water and aqueous ammonia solutions. Plotting (including log-log plots) the effect of the varying concentrations of 2PC12 and 2PC14 on the extraction capability, the authors concluded that the neutral species [CdCl<sub>2</sub>(extractant)<sub>2</sub>] were formed during the liquid-liquid extraction process, allowing the transfer of the complexed toxic metal ion into the organic phase.

2-pyridyl ketoximes (including 2PC12) have also been used for copper(II) extraction from chloride solutions [13].

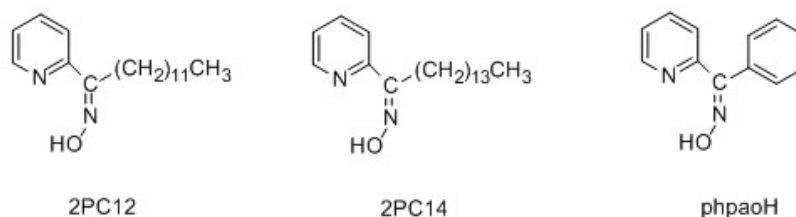


**Figure 1.** Structural formulae of the Cd(II) extractants, 2PC12, 2PC14, and the model ligand phenyl 2-pyridyl ketoxime (phpaoH) used in the present work.

We have embarked on a new program [14] aiming at modeling various aspects of the liquid-liquid extraction of toxic Cd(II) from chloride solutions by 2PC12 and 2PC14 [12], adopting an inorganic (coordination) chemistry approach. In this work, which is the first of a series of papers, we were interested in investigating the existence of the  $[\text{CdCl}_2(2\text{PC12})_2]$  and  $[\text{CdCl}_2(2\text{PC14})_2]$  species that have been proposed to form during the solvent extraction process. The reactions of 2PC12 or 2PC14 with  $\text{CdCl}_2 \cdot 2\text{H}_2\text{O}$  in various organic solvents (ethanol, EtOH; acetonitrile, MeCN;  $\text{CHCl}_3$ ) or organic solvent mixtures (EtOH/MeCN, MeCN/ $\text{CHCl}_3$ ) gave solid products that could not be crystallized for single-crystal X-ray studies. Thus, we used phenyl 2-pyridyl ketoxime [other names: phenyl(pyridin-2-yl)methanone oxime or (N-hydroxy-1-phenyl-2-yl)methanimine] in our synthetic efforts, which gave crystalline complexes. This compound (Figure 1, its abbreviation will be phpaoH in the present work) is a satisfactory analog (albeit not an ideal one) of the extractants 2PC12 and 2PC14. The three ketoximes possess a 2-pyridyl ring, an oxime group, and a hydrophobic substituent on the oxime carbon; the main difference is the presence of a long aliphatic chain in the real extractants instead of the phenyl aromatic ring substituent in phpaoH. This paper describes our results from the synthetic investigation of the general reaction system  $\text{CdCl}_2 \cdot 2\text{H}_2\text{O}/\text{phpaoH}$  and from the full structural and spectroscopic characterization of the products; the implication of our study with respect to the solvent extraction of Cd(II) from aqueous chloride solutions by 2-pyridyl ketoximes have also been critically discussed. The present work can be considered as a continuation of our interest in several aspects of Cd(II) chemistry [15–20] and the coordination chemistry of 2-pyridyl oximes (aldo-, keto-, and amidoximes) [20–33]. Our previous experience on the latter area shows that phpaoH behaves similarly with methyl 2-pyridyl ketoxime (mepaoH; the substituent on the oxime carbon atom is a methyl group) [21,30] in 3d- and mixed 3d/4f-metal complexes, and this justifies partly the choice of phpaoH for our model studies.

## 2. Results and Discussion

### 2.1. Synthetic Comments

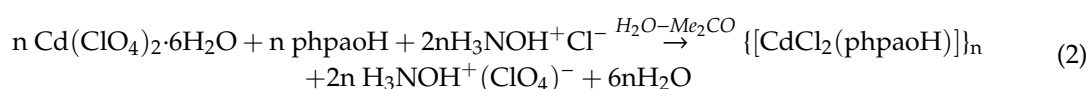
A variety of Cd(II)/Cl<sup>−</sup>/phpaoH reaction systems involving various metal sources, and different reagent ratios, solvent media, and crystallization methods were systematically employed before arriving at the optimized synthetic conditions reported in Section 3. Since all the extraction experiments were carried out in an H<sub>2</sub>O-organic solvent system [12], we used solvent mixtures comprising both H<sub>2</sub>O and an organic solvent, the latter being mixed well with the former. It was not possible to use a two-phase system, e.g., H<sub>2</sub>O- $\text{CHCl}_3$  (as in the real extraction experiments [12]), because of the rather poor solubility of phpaoH in the organic phase. In all the extraction experiments, the pH of the aqueous phases was between 3.5 and 3.8 [12], suggesting that 2PC12 and 2PC14 remain neutral during the process; we thus avoided the addition of an external base (e.g., LiOH, Et<sub>3</sub>N, R<sub>4</sub>NOH, etc.) in the reaction systems. The only solvent mixture that gave crystals of the products (suitable for single-crystal

X-ray crystallography) was the H<sub>2</sub>O-Me<sub>2</sub>CO one. Depending on the reactants molar ratio, two different CdCl<sub>2</sub>/phpaoH products were obtained.

The 1:2 reaction between CdCl<sub>2</sub>·2H<sub>2</sub>O and phpaoH in H<sub>2</sub>O-Me<sub>2</sub>CO (1:1 v/v) gave a colorless solution from which crystals of [CdCl<sub>2</sub>(phpaoH)<sub>2</sub>]·H<sub>2</sub>O (1·H<sub>2</sub>O) were subsequently isolated in rather low yields (~30%). Our efforts to increase the yield by increasing the phpaoH:Cd(II) molar ratio from 2:1 to 3:1 or/and by increasing the H<sub>2</sub>O volume percentage in the solvent mixture resulted in 1·H<sub>2</sub>O contaminated with free phpaoH (analytical and IR evidence). Increase of the Me<sub>2</sub>CO volume percentage did not significantly improve the yield. Assuming that the mononuclear complex is the only product from the reaction system, its formation is summarized by chemical Equation (1).



As mentioned above, the CdCl<sub>2</sub>·2H<sub>2</sub>O:phpaoH molar ratio affected the product identity. The 1:1 reaction between CdCl<sub>2</sub>·2H<sub>2</sub>O and phpaoH in the same solvent mixture used for the preparation of 1·H<sub>2</sub>O, i.e., H<sub>2</sub>O-Me<sub>2</sub>CO (1:1 v/v), gave a microcrystalline powder **A** whose analytical data and IR spectra were different from those of 1·H<sub>2</sub>O; the analytical data fitted well the empirical formula CdCl<sub>2</sub>(phpaoH), suggesting the existence of a 1:1 complex. Keeping constant the solvent mixture, all our efforts to obtain crystals of this 1:1 product were in vain. After hundreds of experiments, the solution of the problem came from a non-orthodox reaction, which involved the use of a chloride-free Cd(II) source and “external” chloride ions. The 1:1:2 Cd(ClO<sub>4</sub>)<sub>2</sub>·6H<sub>2</sub>O/phpaoH/H<sub>3</sub>NOH<sup>+</sup>Cl<sup>-</sup> (hydroxylamine hydrochloride) reaction mixture in H<sub>2</sub>O-Me<sub>2</sub>CO (1:5 v/v) gave a pale yellow solution, which—upon standing undisturbed—gave well-formed colorless crystals of the polymeric complex {[CdCl<sub>2</sub>(phpaoH)]}<sub>n</sub> (**2**) in high yield (~80%). Use of a solvent mixture with a higher H<sub>2</sub>O volume percentage, e.g., H<sub>2</sub>O-Me<sub>2</sub>CO = 1:1, decreased the yield of the reaction and made the quality of single crystals worse. The IR spectrum of **2** was identical with that of **A**, proving that the polymeric compound can also be prepared (albeit in the form of a microcrystalline powder) by using CdCl<sub>2</sub>·2H<sub>2</sub>O as the source of Cd(II). With the results at hand, it is rather difficult to estimate the role of ClO<sub>4</sub><sup>-</sup> ions and hydroxylamine hydrochloride in the formation of product with good crystallinity; we tentatively propose that the higher ionic strength of the Cd(ClO<sub>4</sub>)<sub>2</sub>·6H<sub>2</sub>O/phpaoH/H<sub>3</sub>NOH<sup>+</sup>Cl<sup>-</sup> reaction medium has a positive impact on the quality of the crystals obtained. The formation of the complex, using the method that gave single crystals, is illustrated in the chemical Equation (2).



## 2.2. Description of Structures

The structures of 1·H<sub>2</sub>O and **2** were determined by single-crystal X-ray crystallography. Crystallographic data are listed in Table 1. Various structural plots are shown in Figures 2–6. Selected interatomic distances and angles are given in Tables 2 and 3, while hydrogen bonding details are summarized in Tables 4 and 5.

**Table 1.** Crystallographic data and structural refinement parameters for complexes **1** and **2**.

Parameter	[CdCl <sub>2</sub> (phpaoH) <sub>2</sub> ] $\cdot$ H <sub>2</sub> O(1 $\cdot$ H <sub>2</sub> O)	{[CdCl <sub>2</sub> (phpaoH)] <sub>n</sub> (2)}
Empirical formula	C <sub>24</sub> H <sub>22</sub> CdCl <sub>2</sub> N <sub>4</sub> O <sub>3</sub>	C <sub>12</sub> H <sub>10</sub> CdCl <sub>2</sub> N <sub>2</sub> O
Formula weight	597.75	381.52
Crystal system	monoclinic	triclinic
Space group	<i>P</i> 2 <sub>1</sub> / <i>c</i>	<i>P</i> -1
Color	colorless	colorless
Crystal size, mm	0.49 $\times$ 0.16 $\times$ 0.12	0.27 $\times$ 0.09 $\times$ 0.04
Crystal habit	block-shaped	block-shaped
<i>a</i> , Å	13.6684 (3)	7.0792 (1)
<i>b</i> , Å	8.8598 (2)	8.3260 (1)
<i>c</i> , Å	20.9270 (4)	12.3667 (3)
$\alpha$ , °	90.00	70.652 (1)
$\beta$ , °	106.944 (1)	72.547 (1)
$\gamma$ , °	90.00	85.323 (1)
Volume, Å <sup>3</sup>	2424.23 (9)	655.95 (2)
<i>Z</i>	4	2
Temperature, K	160	160
Radiation, Å	Cu-K $\alpha$ (1.54178)	Cu-K $\alpha$ (1.54178)
Calculated density, g $\cdot$ cm <sup>-3</sup>	1.638	1.932
Absorption coefficient, mm <sup>-1</sup>	9.53	16.99
No. of measured, independent, and observed [ <i>I</i> > 2 $\sigma$ ( <i>I</i> )] reflections	36455, 4072, 3959	8385, 2014, 1855
<i>R</i> <sub>int</sub>	0.047	0.065
Number of parameters	394	164
Final <i>R</i> indices [ <i>I</i> > 2 $\sigma$ ( <i>I</i> )] <sup>a</sup>	<i>R</i> <sub>1</sub> = 0.0267, <i>wR</i> <sub>2</sub> = 0.0665	<i>R</i> <sub>1</sub> = 0.0299, <i>wR</i> <sub>2</sub> = 0.0715
Goodness-of-fit on <i>F</i> <sup>2</sup>	1.10	1.08
Largest differences peak and hole (e Å <sup>-3</sup> )	0.62/−1.26	0.68/−0.87

<sup>a</sup>*R*<sub>1</sub> =  $\Sigma(|F_0| - |F_c|)/\Sigma(|F_0|)$ , *wR*<sub>2</sub> =  $\{\Sigma[w(F_0^2 - F_c^2)^2]/\Sigma[w(F_0^2)^2]\}^{1/2}$ ,  $w = 1/[\sigma^2(F_0^2) + (aP)^2 + bP]$ , where  $P = [\max(F_0^2, 0) + 2F_c^2]/3$  (*a* = 0.0307 and *b* = 3.3484 for 1 $\cdot$ H<sub>2</sub>O; *a* = 0.0256 and *b* = 0.1966 for 2).

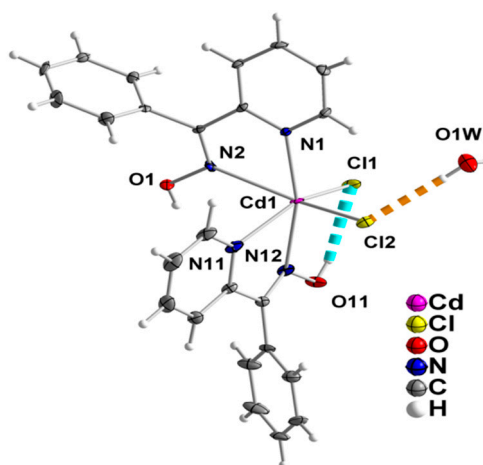


**Figure 2.** The molecules [CdCl<sub>2</sub>(phpaoH)<sub>2</sub>] and H<sub>2</sub>O that are present in the crystal structure of 1 $\cdot$ H<sub>2</sub>O. The thermal ellipsoids are presented at the 50% level. Only diagnostic atoms have been numbered. Dashed lines indicate hydrogen bonds in which the symmetry operation is *x*, *y*, *z*. Through the hydrogen bond indicated with the orange color, molecular pairs of the type {[CdCl<sub>2</sub>(phpaoH)<sub>2</sub>] – H<sub>2</sub>O} are formed in the crystal.

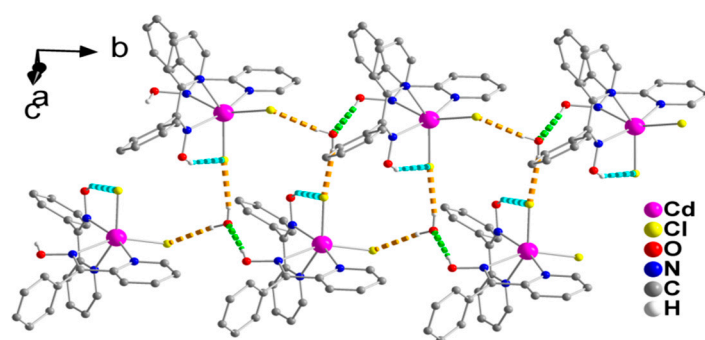


**Figure 3.** A small portion of one double chain, formed through hydrogen bonds, in the crystal structure of  $1 \cdot \text{H}_2\text{O}$ . The dashed light green and dashed cyan lines represent the hydrogen bonds  $\text{O1-H}(\text{O1}) \cdots \text{O1W}(x, -1 + y, z)$  and  $\text{O11-H}(\text{O11}) \cdots \text{Cl1}(x, y, z)$ , respectively. The dashed orange lines represent the hydrogen bonds  $\text{O1W-H}_A(\text{O1W}) \cdots \text{Cl2}(x, y, z)$  and  $\text{O1W-H}_B(\text{O1W}) \cdots \text{Cl1}(-x, 0.5 + y, 0.5 - z)$ . For clarity, only hydrogen atoms involved in hydrogen bonding interactions are shown.

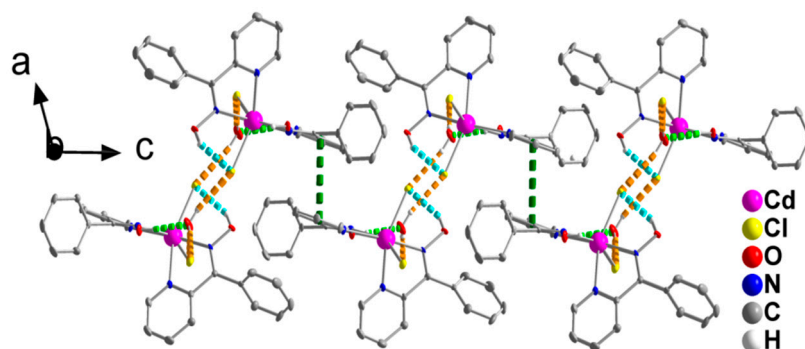


**Figure 4.** Formation of layers parallel to the (001) plane through  $\pi$ - $\pi$  stacking interactions (dashed dark green lines) in the crystal structure of  $1 \cdot \text{H}_2\text{O}$  (see text for details). The view is presented along the  $a$  axis. The color code for the hydrogen bonds is the same as used in Figure 3.

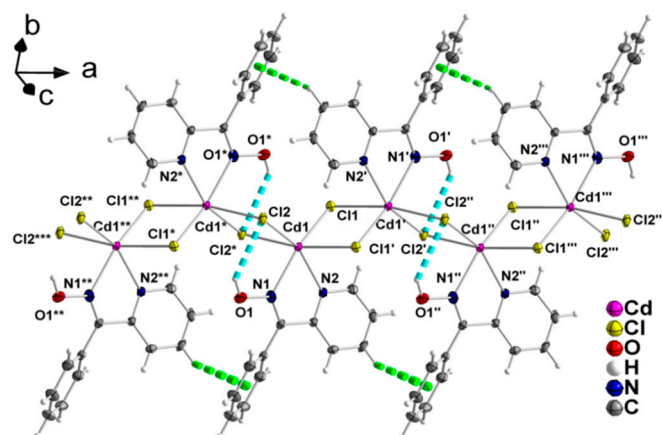


**Figure 5.** A small portion of one zigzag chain formed parallel to the ' $a$ ' axis in the crystal structure of **2**. The thermal ellipsoids are presented at the 50% level. The dashed cyan and light green lines represent  $\text{O1-H}(\text{O1}) \cdots \text{Cl2}$  hydrogen bonds and  $\text{C-H} \cdots \pi$  interactions [ $\text{C3-Cg1}$  3.502(5) Å,  $\text{C3-H}(\text{C3})$  0.950(4) Å,  $\text{H}(\text{C3}) \cdots \text{Cg1}$  2.952(1) Å,  $\text{C3-H}(\text{C3}) \cdots \text{Cg1}$  118.4(3)°], respectively; C3 is a 2-pyridyl carbon atom and Cg1 is the centroid of the phenyl ring of phpaOH. Symmetry codes: (')  $-x + 2, -y + 2, -z + 1$ ; (")  $x + 1, y, z$ ; (""')  $-x + 3, -y + 2, -z + 1$ ; (""")  $x + 2, y, z$ ; (\*)  $-x + 1, -y + 2, -z + 1$ ; (\*\*)  $-x, y, z$ ; (\*\*\*)  $-x, -y + 2, -z + 1$ .



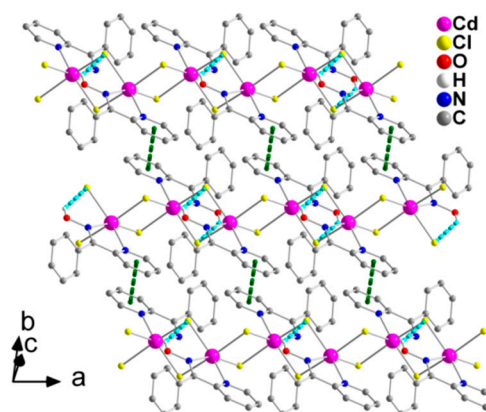


**Figure 6.** Formation of layers parallel to the (001) plane through  $\pi$ - $\pi$  stacking interactions (dashed dark green lines) in the crystal structure of **2**. The C-H $\cdots$  $\pi$  interactions are not shown for clarity reasons. The color code for the hydrogen bonds is the same as used in Figure 5.

**Table 2.** Selected bond lengths (Å) and angles (°) for complex  $[\text{CdCl}_2(\text{phpaoH})_2] \cdot \text{H}_2\text{O}$  ( $1 \cdot \text{H}_2\text{O}$ ).

Bond Lengths (Å)		Bond Lengths (Å)	
Cd1-Cl1	2.532(1)	Cd1-N12	2.373(2)
Cd1-Cl2	2.534(1)	N2-O1	1.387(3)
Cd1-N1	2.323(2)	N12-O11	1.381(3)
Cd1-N2	2.509(2)	C6 <sup>a</sup> -N2	1.286(3)
Cd1-N11	2.405(2)	C26 <sup>a</sup> -N12	1.278(3)
Angles (°)		Angles (°)	
N1-Cd1-N2	69.8 (1)	N11-Cd1-N12	67.3 (1)
N1-Cd1-N11	105.3 (1)	N11-Cd1-Cl1	149.4 (1)
N1-Cd1-N12	166.2 (1)	N11-Cd1-Cl2	87.3 (1)
N1-Cd1-Cl1	102.1 (1)	N12-Cd1-Cl1	83.0 (1)
N1-Cd1-Cl2	92.3 (1)	N12-Cd1-Cl2	98.9 (1)
N2-Cd1-N11	80.2 (1)	Cl1-Cd1-Cl2	105.0 (1)
N2-Cd1-N12	98.9 (1)	C6 <sup>a</sup> -N2-O1	112.9 (2)
N2-Cd1-Cl1	98.1 (1)	C26 <sup>a</sup> -N12-O11	115.6 (2)
N2-Cd1-Cl2	152.3 (1)		

<sup>a</sup> Atoms C6 and C26 (not labeled in Figure 2) are the oxime carbon atoms.

The crystal structure of  $1 \cdot \text{H}_2\text{O}$  consists of complex molecules  $[\text{CdCl}_2(\text{phpaoH})_2]$  and lattice  $\text{H}_2\text{O}$  molecules in a 1:1 ratio. The  $\text{Cd}^{\text{II}}$  atom is coordinated by two chloro (or chlorido) groups (Cl1, Cl2), two oxime nitrogen atoms (N2, N12), and two 2-pyridyl nitrogen atoms (N1, N11), the latter four arising from two  $N,N'$ -bidentate chelating (or 1.011 adopting the Harris notation [34])  $\text{phpaoH}$  ligands. The coordination geometry of the metal ion is distorted octahedral, the *trans* and *cis* donor atom - $\text{Cd}^{\text{II}}$ -donor atom bond angles being in the ranges  $149.4(1)$ – $166.2(1)^\circ$  and  $67.3(1)$ – $105.3(1)^\circ$ , respectively. The distortion from the regular octahedral geometry is primarily attributed to the small bite angles of the two 5-membered chelating rings [ $\text{N1-Cd1-N2} = 69.8(1)^\circ$ ,  $\text{N11-Cd1-N12} = 67.3(1)^\circ$ ]. The octahedral molecule is the *cis-cis-cis* isomer considering the positions of the chloro ligands, the oxime, and the 2-pyridyl nitrogen donor atoms. There is one intramolecular hydrogen bond of medium strength with the uncoordinated oxime oxygen atom O11 as a donor and the coordinated chloride Cl1 as acceptor. Through the  $\text{O1W-H}_A(\text{O1W}) \cdots \text{Cl2}$  “intramolecular” hydrogen bond, each lattice  $\text{H}_2\text{O}$  molecule is associated with one  $[\text{CdCl}_2(\text{phpaoH})_2]$  molecule and molecular  $\{[\text{CdCl}_2(\text{phpaoH})_2] \cdot \text{H}_2\text{O}\}$  pairs are thus formed in the crystal; this view is emphasized in Figure 2.

**Table 3.** Selected interatomic distances (Å) and angles (°) for complex  $\{[\text{CdCl}_2(\text{phpaoH})]\}_n$  (2)<sup>a</sup>.

Interatomic Distances (Å)		Interatomic Distances (Å)	
Cd1...Cd1'	3.871 (1)	Cd1-Cl2*	2.686 (1)
Cd1...Cd1*	3.978 (1)	Cd1-N1	2.407 (4)
Cd1-Cl1	2.564 (1)	Cd1-N2	2.323 (3)
Cd1-Cl1'	2.682 (1)	C6 <sup>b</sup> -N1	1.293 (5)
Cd1-Cl2	2.575 (1)	N1-O1	1.386 (4)
Angles (°)		Angles (°)	
N1-Cd1-N2	67.6(1)	Cl1-Cd1-Cl2	112.6(1)
N1-Cd1-Cl1	160.1(1)	Cl1-Cd1-Cl2*	87.5(1)
N1-Cd1-Cl1'	101.4(1)	Cl1'-Cd1-Cl2	93.1(1)
N1-Cd1-Cl2	86.1(1)	Cl1'-Cd1-Cl2*	168.4(1)
N1-Cd1-Cl2*	88.7(1)	Cl2-Cd1-Cl2*	81.8(1)
N2-Cd1-Cl1	97.8(1)	Cd1-Cl1-Cd1'	95.1(1)
N2-Cd1-Cl1'	83.3(1)	Cd1-Cl2-Cd1*	98.3(1)
N2-Cd1-Cl2	152.0(1)	C6 <sup>b</sup> -N1-O1	114.5(4)
N2-Cd1-Cl2*	106.2(1)	Cd1-N1-O1	123.9(2)
Cl1-Cd1-Cl1'	84.9(1)	Cd1-N1-C6 <sup>b</sup>	120.5(3)

<sup>a</sup> Symmetry codes: (')  $-x + 2, -y + 2, -z + 1$ ; (\*)  $-x + 1, -y + 2, -z + 1$ . <sup>b</sup> Atom C6 (not labeled in Figure 5) is the oxime carbon atom.

**Table 4.** Hydrogen bonding interactions (Å, deg) in the crystal structure of  $[\text{CdCl}_2(\text{phpaoH})_2] \cdot \text{H}_2\text{O}$  (1·H<sub>2</sub>O).

D-H...A	d(D...A)	d(D-H)	d(H...A)	<DHA	Symmetry Code of A
O11-H(O11)...Cl1	3.098(2)	0.77(4)	2.38(4)	155(3)	$x, y, z$
O1W-H <sub>A</sub> (O1W)...Cl2	3.122(3)	0.80(5)	2.33(5)	174(4)	$x, y, z$
O1W-H <sub>B</sub> (O1W)...Cl1	3.241(2)	0.85(4)	2.41(5)	165(4)	$-x, 0.5+y, 0.5-z$
O1-H(O1)...O1W	2.623(3)	0.76(3)	1.87(3)	170(3)	$x, -1+y, z$

D = donor; A = acceptor.

**Table 5.** Hydrogen bonding interactions (Å, deg) in the crystal structure of  $\{[\text{CdCl}_2(\text{phpaoH})]\}_n$  (2).

D-H...A	d(D...A)	d(D-H)	d(H...A)	<DHA	Symmetry Code of A
O1-H(O1)...Cl2	3.379(3)	0.84	2.69	140	$x, y, z$
O1-H(O1)...Cl1*	3.378(3)	0.84	2.74	133	$-x + 1, -y + 2, -z + 1$

D = donor; A = acceptor.

The complex  $[\text{CdCl}_2(\text{phpaoH})_2]$  and solvent H<sub>2</sub>O molecules form double chains (1D), which are parallel to the *b* axis (Figure 3) through O1-H(O1)...O1W, O1W-H<sub>A</sub>(O1W)...Cl2, and O1W-H<sub>B</sub>(O1W)...Cl1 H bonds. Each lattice H<sub>2</sub>O is connected to three complex molecules.

The double chains in the structure of 1·H<sub>2</sub>O are further linked through  $\pi$ - $\pi$  stacking interactions between centrosymmetrically-related 2-pyridyl rings containing the N1 atom, forming layers parallel to the (001) plane (Figure 4). The centroid...centroid distance between the parallel aromatic rings is 3.761 Å.

Compound 2 is a 1D coordination polymer. Its crystal structure consists of zigzag chains extended parallel to the crystallographic 'a' axis (Figure 5). The Cd<sup>II</sup> atoms are doubly bridged by two asymmetric  $\mu$ -chloro groups. One *N,N'*-bidentate chelating (1.011) phpaoH ligand completes six-coordination at each metal ion. The Cd<sup>II</sup> coordination polyhedron is a distorted octahedron. The *trans* coordination angles are in the 152.0 (1)–168.4 (1)° range, while the *cis* ones are in the 67.6 (1)–112.6 (1)° range. There are rather weak, intrachain hydrogen bonds in which the oxime oxygen atom O1 is the donor and



the bridging chloro groups Cl2 and Cl1 are the acceptors; only the O1-H(O1)⋯Cl2 component of this bifurcated hydrogen bond is shown in Figure 5.

The 1D polymeric chains in the crystal structure of **2** are further linked through weak  $\pi$ - $\pi$  stacking interactions between centrosymmetrically-related 2-pyridyl rings, forming layers that extend parallel to the (001) plane (Figure 6). The centroid⋯centroid distance between the aromatic heterocyclic rings is 4.079 Å. In addition, there is a C-H⋯ $\pi$  interaction, in which a pyridyl carbon atom (C3) is the donor and the phenyl ring (C7–C12) of phpaoH is the acceptor.

The Cd-Cl bond lengths in **1**·H<sub>2</sub>O [2.532(1) and 2.534(1) Å] are shorter than those in **2** [2.564(1)–2.686(1) Å] due to the terminal character of the chloro ligands in the former versus the bridging one in the latter. The bridging Cd-Cl bond distances in **2** are typical for other six-coordinate Cd(II) complexes containing bridging chloro groups [15]. The carbon-nitrogen [1.278(3)–1.293(5) Å] and nitrogen-oxygen [1.381(3)–1.387(3) Å] bond lengths of the coordinated oxime groups are similar (for a given bond type) in the two complexes; the nitrogen-oxygen bonds are longer than the carbon-nitrogen bonds due to their different multiplicity (single versus double). The carbon-nitrogen and nitrogen-oxygen bond lengths in the two complexes are practically similar and slightly larger, respectively, compared with the corresponding bond distances observed in the crystal structures of the various polymorphs of the free phpaoH [35–37].

Complexes **1**·H<sub>2</sub>O and **2** are new members in the large family of metal complexes with the neutral phpaoH or its deprotonated form (phpao<sup>−</sup>) as ligands [21,24,27,29,30,32,38–46]; only representative references are listed. The only structurally characterized Cd(II)/phpaoH species to-date is the cationic octahedral complex [Cd(phpaoH)<sub>3</sub>](NO<sub>3</sub>)<sub>2</sub> [46], prepared by the 1:2 reaction of Cd(NO<sub>3</sub>)<sub>2</sub>·4H<sub>2</sub>O and phpaoH. The Cd-N bond lengths [2.320(3)–2.402(3) Å] in this complex are similar with those of **1**·H<sub>2</sub>O and **2** [2.323(2)–2.509(2) Å]. The polymeric structural type of **2** is completely new in the coordination chemistry of phpaoH. There have been only two mononuclear complexes reported with the formula [M<sup>II</sup>Cl<sub>2</sub>(phpaoH)<sub>2</sub>] (M<sup>II</sup> = a divalent metal), namely [NiCl<sub>2</sub>(phpaoH)<sub>2</sub>]·Me<sub>2</sub>CO [42] and [MnCl<sub>2</sub>(phpaoH)<sub>2</sub>]·0.02EtOH [43]; both compounds contain *cis-trans-cis* octahedral molecules considering the positions of the chloro groups, the oxime nitrogen atoms, and the 2-pyridyl nitrogen atoms, respectively. Complex **1**, with a *cis-cis-cis* disposition of the chemically similar donors, is thus a unique geometrical isomer in the [M<sup>II</sup>Cl<sub>2</sub>(phpaoH)<sub>2</sub>] series.

### 2.3. Spectroscopic Studies

We discuss first the vibrational spectra of **1**·H<sub>2</sub>O and **2**. The FT-Raman spectra of the free compound phpaoH and its Cd(II) complexes **1**·H<sub>2</sub>O and **2** are presented in Figure 7.

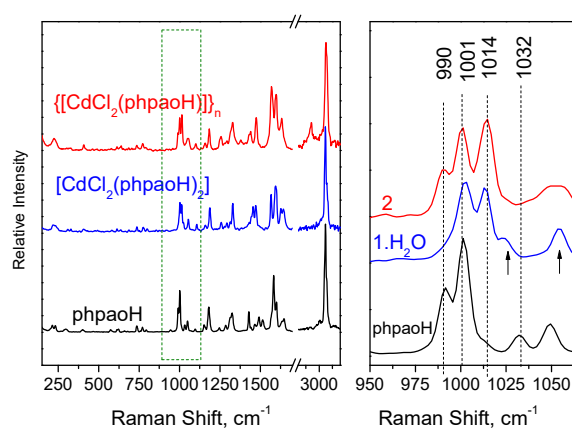


**Figure 7.** The FT-Raman spectra of compounds phpaoH, **1**·H<sub>2</sub>O, and **2**.

In the solid-state (KBr) IR spectrum of **1**·H<sub>2</sub>O, the medium-intensity band at 3506 cm<sup>−1</sup> and the weak band at 1628 cm<sup>−1</sup> are attributed to the  $\nu$ (OH) and  $\delta$ (HOH) vibrations, respectively, of the lattice

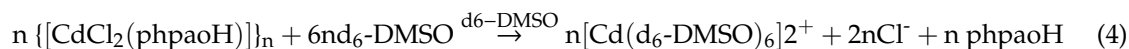
water that is present in the complex [47]. The rather high wavenumber of the stretching vibration is indicative of the non-coordinating nature of the H<sub>2</sub>O molecule. These bands are absent from the IR spectra of phpaoH and **2**. The presence of neutral oxime groups in the complexes is manifested by the appearance of a medium-to-strong IR band at 3384 (1·H<sub>2</sub>O) and 3388 (**2**) cm<sup>-1</sup> assigned to the  $\nu(\text{OH})$  vibration [48,49]. The corresponding band in the spectrum of the free ligand appears at 3154 cm<sup>-1</sup>. The large wavenumber difference can be explained by the involvement of the -OH group in hydrogen bonds of different strength in the complexes and in the free phpaoH compound. As expected, the  $\nu(\text{OH})$  peaks are hardly seen in the Raman spectra. On the contrary, at the high-frequency part of the Raman spectra, the strong peaks at 3060 (1·H<sub>2</sub>O) and 3064 (**2**) are assigned to a  $\nu(\text{C-H})$  vibration [50]. The medium-intensity bands at 1568 and 1094 cm<sup>-1</sup> in the IR spectrum of the free ligand phpaoH have been assigned [40,48] to the  $\nu(\text{C=N})$  and  $\nu(\text{N-O})$  vibrations of the oxime group, respectively. The 1094 cm<sup>-1</sup> band is shifted to a lower wavenumber in the spectra of the complexes (1054 cm<sup>-1</sup> in 1·H<sub>2</sub>O, 1042 cm<sup>-1</sup> in **2**). This shift has been attributed to the coordination of the neutral oxime nitrogen [40,48]. To our surprise, the 1568 cm<sup>-1</sup> band is shifted to a higher wavenumber in the IR spectra of the complexes (1590 cm<sup>-1</sup> in 1·H<sub>2</sub>O, 1600 cm<sup>-1</sup> in **2**), overlapping with an aromatic stretching vibration [48]. This experimental fact is not unusual [48]. Extensive studies on complexes with ligands containing a C=N bond (with the carbon atom attached to an aromatic ring) have shown [51] that a change in the s character of the N lone pair occurs upon coordination and the s character of the nitrogen orbital involved in the C=N bond increases; this change in hybridization leads to a greater C=N stretching force constant relative to the free neutral ligands, thus shifting the  $\nu(\text{C=N})$  band in the spectra of the complexes to higher wavenumbers. The Raman  $\nu(\text{C=N})$  peaks for phpaoH, 1·H<sub>2</sub>O, and **2** appear at 1599, 1626, and 1631 cm<sup>-1</sup>, respectively [50,52,53], while the  $\nu(\text{N-O})$  peaks appear at 1097 (phpaoH), 1053 (1·H<sub>2</sub>O), and 1052 (**2**) cm<sup>-1</sup>, respectively [53]. The Raman coordination shifts are in the same directions with the corresponding IR ones. The medium-intensity peaks in the Raman spectra of the free ligand and the two complexes at ~1330 cm<sup>-1</sup> are attributed to the NOH in-plane deformation,  $\delta(\text{NOH})$  [50].

The in-plane deformation band of the 2-pyridyl ring,  $\delta(\text{py})$ , in the IR spectrum of free phpaoH at 622 cm<sup>-1</sup> shifts to higher wavenumbers (~660 cm<sup>-1</sup>) in the spectra of the complexes, confirming the participation of the heterocyclic nitrogen atom in coordination [48]. This mode appears [50] at 622, 636, and 639 cm<sup>-1</sup> in the Raman spectra of phpaoH, 1·H<sub>2</sub>O, and **2**, respectively. The Raman peaks in the 410–210 cm<sup>-1</sup> region are associated with the Cd-Cl, Cd-N(pyridyl), and Cd-N(oxime) stretching vibrations [54].

The specific spectral window of the FT-Raman spectra, where major spectral changes occur, is separately shown in Figure 7, right. These spectral changes are attributed to pyridine ring-breathing vibrations [49]. Compound phpaoH exhibits Raman peaks at 990 and 1032 cm<sup>-1</sup> assigned to totally symmetric ring-breathing and trigonal ring deformation modes, respectively [50,55,56]. In both 1·H<sub>2</sub>O and **2**, a new Raman band appears at 1014 cm<sup>-1</sup>. Similar behavior has been observed (a) for complexes with the formulae NiCl<sub>2</sub>(py)<sub>2</sub> and CoCl<sub>2</sub>(py)<sub>2</sub> relative to the spectrum of pyridine (py), and (b) after adsorption of pyridine on transition metal electrodes [57]. A note is made of the fact that the Raman band at ~1000 cm<sup>-1</sup> is characteristic of the mono-substituted benzene ring.

The <sup>1</sup>H NMR spectra of 1·H<sub>2</sub>O and **2** in d<sub>6</sub>-DMSO are identical. The most remarkable feature is that the spectra are almost identical with the spectrum of free phpaoH in the same solvent. The spectra show a singlet signal at  $\delta$  11.61 ppm assigned to the hydroxyl proton [14,58,59] and a doublet at  $\delta$  8.49 ppm attributed to the proton of the aromatic carbon adjacent to the ring N-atom [14,24]. The other 2-pyridyl protons and the phenyl protons appear in the region  $\delta$  7.88–7.29 ppm. This experimental fact indicates that the two complexes decompose in solution, probably as indicated by equations (3) and (4). Strong evidence from our proposal comes from the molar conductivity values,  $\Lambda_M$  (10<sup>-3</sup> M, 25 °C), for the two complexes in DMSO, which are 73 (1·H<sub>2</sub>O) and 82 (**2**) S cm<sup>2</sup> mol<sup>-1</sup>, indicative of 1:2 electrolytes [60]. The <sup>1</sup>H-NMR spectra of 1·H<sub>2</sub>O and **2** in CD<sub>3</sub>OD are complicated, suggesting the presence of 2–3 species in equilibrium. For both complexes, at least one species contains coordinated

phpaoH, as evidenced from the downfield shift of the doublet signal due to the proton of the aromatic carbon adjacent to the 2-pyridyl nitrogen atom, which appears at  $\delta \sim 8.8$  ppm.



### 3. Experimental Section

#### 3.1. Materials and Physical-Spectroscopic Measurements

All manipulations were performed under aerobic conditions. Reagents and solvents were purchased from Alfa Aesar (Karlsruhe, Germany) and Aldrich (Tanfrichen, Germany) and used as received. The free ligand phenyl 2-pyridyl ketoxime (phpaoH) was synthesized as described in the literature [58] in a >80% yield; its purity was checked by  $^1\text{H-NMR}$  spectroscopy and the determination of its melting point (found, 148–149 °C; reported, 149–151 °C).

Elemental analyses (C, H, N) were performed by the University of Patras Center for Instrumental Analysis. Conductivity measurements were carried out at 25 °C with a Metrohm-Herisau E-527 bridge (Herisau, Switzerland) and a cell of standard constant. FT-IR spectra were recorded using a Perkin-Elmer 16PC spectrometer (Perkin-Elmer, Waltham, MA, USA) with samples in the form of KBr pellets. FT-Raman spectra were obtained using a Bruker (D) FRA-106/S component (Bruker, Karlsruhe, Germany) attached to an EQUINOX 55 spectrometer. An R510 diode-pumped Nd:YAG laser at 1064 nm was used for Raman excitation with a laser power 250 mW on the sample, utilizing an average of 100 scans at 4  $\text{cm}^{-1}$  resolution.  $^1\text{H NMR}$  spectra were recorded on a 400 MHz Bruker Avance DPX spectrometer (Bruker AVANCE, Billerica, MA, USA) using  $(\text{Me})_4\text{Si}$  as an internal standard.

#### 3.2. Syntheses of the Complexes

$[\text{CdCl}_2(\text{phpaoH})_2] \cdot \text{H}_2\text{O} (1 \cdot \text{H}_2\text{O})$ : A solution of phpaoH (0.079 g, 0.40 mmol) in  $\text{Me}_2\text{CO}$  (6 mL) was added to an aqueous solution (6 mL) of  $\text{CdCl}_2 \cdot 2\text{H}_2\text{O}$  (0.043 g, 0.20 mmol). The resulting slurry was stirred for 20 min, filtered (to remove a small quantity of a white powder), and the filtrate was stored in a closed flask at room temperature. X-ray quality, colorless crystals of the product were obtained within 24 h. The crystals were collected by filtration, washed with EtOH (2 mL) and  $\text{Et}_2\text{O}$  ( $2 \times 2$  mL), and dried in air. Yield: 31%. Anal. Calcd. (%) for  $\text{C}_{24}\text{H}_{22}\text{N}_4\text{CdCl}_2\text{O}_3$ : C, 48.22; H, 3.72; N, 9.37. Found (%): C, 48.48; H, 3.58; N, 9.33. IR (KBr,  $\text{cm}^{-1}$ ): 3506m, 3384m, 3198wb, 3084w, 3060w, 3006w, 2850w, 1628m, 1590m, 1566w, 1470m, 1456s, 1442s, 1432sh, 1330m, 1294w, 1256m, 1186m, 1164m, 1122w, 1106w, 1072sh, 1054s, 1044sh, 1026s, 1014s, 958s, 922w, 912w, 898sh, 848m, 796s, 778m, 738w, 658m. Raman ( $\text{cm}^{-1}$ ): 3082sh, 3073sh, 3060s, 1642m, 1626m, 1594s, 1565s, 1470m, 1454m, 1328m, 1312w, 1292w, 1277w, 1257w, 1187m, 1160w, 1106w, 1053m, 1012m, 1002m, 799w, 775w, 735w, 636w, 612w, 582w, 405w, 327w, 307w, 233sh, 217w.  $^1\text{H-NMR}$  ( $d_6\text{-DMSO}$ ,  $\delta/\text{ppm}$ ): 11.61(s,2H), 8.49(d,2H), 7.85(mt,4H), 7.39(mt,8H), 7.30(dd,4H), 3.35(s, protons of the lattice  $\text{H}_2\text{O}$  and  $\text{H}_2\text{O}$  contained in the deuterated solvent).

$\{[\text{CdCl}_2(\text{phpaoH})]\}_n (2)$ : A slurry of phpaoH (0.040 g, 0.20 mmol),  $\text{Cd}(\text{ClO}_4)_2 \cdot 6\text{H}_2\text{O}$  (0.084 g, 0.20 mmol), and  $\text{H}_3\text{NOH}^+ \text{Cl}^-$  (0.028 g, 0.40 mmol) in  $\text{Me}_2\text{CO}$  (5 mL) was stirred for 5 min.  $\text{H}_2\text{O}$  (1 mL) was then added to the slurry, and the resulting pale yellow solution was stirred for a further 5 min and stored in a closed flask at room temperature. X-ray quality, colorless crystals of the product were precipitated after 10 d. The crystals were collected by filtration, washed with  $\text{Et}_2\text{O}$  ( $3 \times 1$  mL), and dried in air. Yield: 79%. Anal. Calcd. (%) for  $\text{C}_{12}\text{H}_{10}\text{N}_2\text{OCdCl}_2$ : C, 37.77; H, 2.65; N, 7.34. Found (%): C, 37.95; H, 2.57; N, 7.50. IR (KBr,  $\text{cm}^{-1}$ ): 3388sb, 3056w, 3024w, 2896w, 1600m, 1540m, 1474m, 1448sh, 1436m, 1376m, 1328m, 1292w, 1260w, 1182m, 1162sh, 1102m, 1080sh, 1062sh, 1042s, 1022s, 954m, 928sh, 898w, 792m, 768w, 750w, 734w, 698s, 658m, 640w, 578w, 550w, 490w, 446w, 422w. Raman ( $\text{cm}^{-1}$ ): 3074sh, 3064s, 2925w, 1631m, 1597s, 1569s, 1474m, 1440w, 1430sh, 1378w, 1328m, 1293w, 1256w,

1184m, 1157w, 1101w, 1052w, 1015m, 1002m, 773w, 735w, 639w, 614w, 408w, 224w.  $^1\text{H-NMR}$  ( $d_6$ -DMSO,  $\delta/\text{ppm}$ ): 11.60(sb,1H), 8.50(d,1H), 7.86(mt,2H), 7.39(mt,4H), 7.29(dd,2H).

### 3.3. Single-Crystal X-ray Crystallography

Colorless crystals of  $1\cdot\text{H}_2\text{O}$  ( $0.12 \times 0.16 \times 0.49$  mm) and **2** ( $0.04 \times 0.09 \times 0.27$  mm) were taken from the mother liquor and immediately cooled to 160 K. Diffraction data were collected on a Rigaku R-Axis Image Plate (Rigaku Americas Corporation, The Woodlands, TX, USA) diffractometer using graphite-monochromated Cu  $K\alpha$  radiation. Data collection ( $\omega$ -scans) and processing (cell refinement, data reduction, and empirical absorption correction) were performed using the CrystalClear program [61]. The structures were solved by direct methods using SHELXS, ver. 2013/1 [62] and refined by full-matrix least-squares techniques on  $F^2$  with SHELXL, ver. 2014/6 [63]. All non-H atoms were refined anisotropically. The H atoms in the structure of  $1\cdot\text{H}_2\text{O}$  were located by different maps and refined isotropically. The H atoms in the structure of **2** were introduced at calculated positions and refined as riding on their corresponding bonded atoms. Plots of the structures were drawn using the Diamond 3 program package [64]. Further crystallographic details for  $1\cdot\text{H}_2\text{O}$ :  $2\theta_{\text{max}} = 130^\circ$ ;  $(\Delta/\sigma)_{\text{max}} = 0.001$ ;  $R_1/wR_2$  (for all data) = 0.0276/0.0672. For **2**:  $2\theta_{\text{max}} = 130^\circ$ ;  $(\Delta/\sigma)_{\text{max}} = 0.001$ ;  $R_1/wR_2$  (for all data) = 0.0325/0.0728.

Crystallographic data have been deposited with the Cambridge Crystallographic Data Center, Nos 1912320 ( $1\cdot\text{H}_2\text{O}$ ) and 1912319 (**2**). Copies of the data can be obtained free of charge upon application to CCDC, 12 Union Road, Cambridge, CB2 1EZ, UK: Telephone: +(44)-1223-762910; Fax: +(44)-1223-336033; E-mail: deposit@ccdc.cam.ac.uk, or via <http://www.ccdc.cam.ac.uk/conts/retrieving.html>.

## 4. Concluding Comments and Perspectives

It is rather difficult to conclude on a project that has not been finished. We have partly fulfilled the goals mentioned in Section 1 (Introduction). With the drawbacks already mentioned (we have not worked with 2PC12 and 2PC14, which have been used in the extraction experiments but, instead, with phpaoH; we have not used  $\text{H}_2\text{O-CHCl}_3$  solvent systems but, instead,  $\text{H}_2\text{O-Me}_2\text{CO}$ ), we believe that complex  $1\cdot\text{H}_2\text{O}$  models satisfactorily the species  $[\text{CdCl}_2(2\text{PC12})_2]$  and  $[\text{CdCl}_2(2\text{PC14})_2]$  that have been proposed to form during the solvent extraction of the toxic Cd(II) from chloride-containing aqueous environments using the extractants 2PC12 and 2PC14. The characterization of **1** proves that neutral complexes  $[\text{CdCl}_2(\text{extractant})_2]$  are capable of existence, favoring the transfer of the toxic metal ion into the organic phase. Our synthetic studies have also led to the 1:1 polymeric compound **2**. The isolation of this complex, albeit with a different 2-pyridyl ketoxime than the real extractants, suggests that polymeric 1:1  $\text{CdCl}_2$ -2PC12 and  $\text{CdCl}_2$ -2PC14 might exist. This explains the experimental fact that the extraction of Cd(II) increases upon an increase in the concentration of extractant [12]; it is obvious that such polymeric complexes should be avoided during the extraction process because their solubility in the organic phase might be low, disfavoring the % extraction.

From the synthetic inorganic chemistry viewpoint, our results emphasize the dramatic influence of the  $\text{CdCl}_2$ :phpaoH molar ratio used on the product identity (monomeric vs. polymeric) and show that the structural chemistry of the  $\text{CdCl}_2$ -phpaoH system is interesting in both molecular and supramolecular levels.

With the valuable knowledge obtained in this study, we have been trying to understand the molecular basis of other interesting phenomena that take place during the solvent extraction of toxic Cd(II) from  $\text{Cl}^-$ -containing aqueous media. Among our future goals are: (1) The preparation and characterization of the species  $[\text{Cd}(\text{NO}_3)_2(\text{extractant})_2]$  and/or  $[\text{CdCl}(\text{NO}_3)(\text{extractant})_2]$  that have been proposed to form during the Cd(II) extraction from aqueous solutions containing low chloride concentrations (<1.0 M) and high nitrate (>3.0 M) concentrations using 2PC12 and 2PC14; (2) the understanding of the negative effect of the increase of the chloride concentration in the aqueous phase on Cd(II) extraction by preparing anionic complexes, e.g.,  $\{(\text{oximeH})[\text{CdCl}_3]\}_n$  and/or  $(\text{oximeH})_2[\text{CdCl}_4]$ ;

(3) the study of the inability of 4-pyridyl ketoximes (e.g., 4PC12 and 4PC14, which are the analogs of 2PC12 and 2PC14, respectively, but with the oxime group on the position 4 of the pyridyl ring) by investigating  $\text{CdCl}_2 \cdot 2\text{H}_2\text{O}/4$ -pyridyl ketoxime complexes. Last, but not least, we have been using 2-pyridyl ketoximes with aliphatic substituents on the carbon atom for reactions with  $\text{Cd(II)}$ ; such ligands are more realistic models of the 2PC12 and 2PC14 extractants.

**Author Contributions:** E.C.M. and V.A. contributed towards the syntheses, crystallization, and conventional characterization of the complexes. Both also contributed to the interpretation of the results. A.S.B., G.A.V., and C.G.E. performed the Raman and  $^1\text{H-NMR}$  experiments, also contributing to their interpretation. A.T. and V.P. collected single-crystal X-ray crystallographic data, solved the structures, and performed their refinements; the latter also studied in detail the supramolecular features of the crystal structures and wrote the relevant part of the paper. G.A.V. and S.P.P. coordinated the research and wrote the paper based on the reports of their collaborators. All the authors exchanged opinions concerning the progress of the project and commented on the writing of the manuscript at all stages.

**Funding:** We acknowledge support of this work by the project MIS 5002772, implemented under the Action “Reinforcement of the Research and Innovation Infrastructure”, funded by the Operational Programme “Competitiveness, Entrepreneurship and Innovation” (NSRF 2014-2020) and co-financed by Greece and the European Union (European Regional Development Fund).

**Acknowledgments:** The authors thank the MSc program “Analytical Chemistry and Nanotechnology” of the Chemistry Department of the University of Patras (Patras, Greece) for providing us with funding for the purchase of few consumables.

**Conflicts of Interest:** The authors declare no conflict of interest.

## References

1. Zahra, M.; Zulfiqar, S.; Skene, W.G.; Sarwar, M.I. Efficient uptake of  $\text{Cd(II)}$  and  $\text{Pb(II)}$  ions by aromatic polyamidoximes. *Ind. Eng. Chem. Res.* **2018**, *57*, 15243–15253. [[CrossRef](#)]
2. Tang, W.W.; Zeng, G.M.; Gong, J.L.; Liang, J.; Xu, P.; Zhang, C.; Huang, B.B. Impact of humic/fulvic acid on the removal of heavy metals from aqueous solutions using nanomaterials: A review. *Sci. Total Env.* **2014**, *468*, 1014–1027. [[CrossRef](#)] [[PubMed](#)]
3. Dakanali, M.; Kefalas, E.T.; Raptopoulou, C.P.; Terzis, A.; Mavromoustakos, T.; Salifoglou, A. Synthesis and spectroscopic and structural studies of a new cadmium(II)-citrate aqueous complex. Potential relevance to cadmium(II)-citrate speciation and links to cadmium toxicity. *Inorg. Chem.* **2003**, *42*, 2531–2537. [[CrossRef](#)] [[PubMed](#)]
4. Kefalas, E.T.; Dakanali, M.; Panagiotidis, P.; Raptopoulou, C.P.; Terzis, A.; Mavromoustakos, T.; Kyrikou, I.; Karligiano, N.; Bino, A.; Salifoglou, A. pH-specific aqueous synthetic chemistry in the binary cadmium(II)-citrate system. Gaining insight into cadmium(II)-citrate speciation with relevance to cadmium toxicity. *Inorg. Chem.* **2005**, *44*, 4818–4828. [[CrossRef](#)] [[PubMed](#)]
5. Manahan, S. *Toxicological Chemistry*; Lewis Publishers, Inc.: Chelsea, MI, USA, 1992.
6. Shiraishi, T.; Tamada, M.; Saito, K.; Sugo, T. Recovery of cadmium from waste of scallop processing with amidoxime adsorbent synthesized by graft-polymerization. *Radiat. Phys. Chem.* **2003**, *66*, 43–47. [[CrossRef](#)]
7. Abdel-Rahman, L.H.; Abu-Dief, A.M.; Abd-El Sayed, M.A.; Zikry, M.M. Disposal of heavy transition  $\text{Cd}^{2+}$  ions from aqueous solution utilizing nanosized flamboyant pod (*Delonix regia*). *J. Transit. Met. Complexes* **2018**, *1*, 236055. [[CrossRef](#)]
8. Tasker, P.A.; Tong, C.C.; Westra, A.N. Co-extraction of cations and anions in base metal recovery. *Coord. Chem. Rev.* **2007**, *251*, 1868–1877. [[CrossRef](#)]
9. Yordanov, A.T.; Roundhill, D.M. Solution extraction of transition and post-transition heavy and precious metals by chelate and macrocyclic ligands. *Coord. Chem. Rev.* **1998**, *170*, 93–124. [[CrossRef](#)]
10. Cotton, F.A.; Wilkinson, G.; Murillo, C.A.; Bochmann, M. *Advanced Inorganic Chemistry*, 3rd ed.; Wiley: New York, NY, USA, 1999; pp. 27–31.
11. Tomaszewska, M.; Borowiak-Resterna, A.; Olszanowski, A. Cadmium extraction from chloride solutions with model *N*-alkyl and *N,N*-dialkyl-pyridine-carboxamides. *Hydrometallurgy* **2007**, *85*, 116–126. [[CrossRef](#)]
12. Parus, A.; Wieszczycka, K.; Olszanowski, A. Solvent extraction of cadmium(II) from chloride solutions by pyridyl ketoximes. *Hydrometallurgy* **2011**, *105*, 284–289. [[CrossRef](#)]



13. Klonowska-Wieszczycza, K.; Olszanowski, A.; Parus, A.; Zydorczak, B. Removal of copper(II) from chloride solutions using hydrophobic pyridyl ketone oximes. *Solvent Extr. Ion Exch.* **2009**, *27*, 50–62. [[CrossRef](#)]
14. Angelidou, V. Modelling the Removal of Cadmium Ions from Wastes Using 2-Pyridyl Oximes. Master's Thesis, University of Patras, Patras, Greece, 2013.
15. Katsoulakou, E.; Konidaris, K.F.; Terzis, A.; Raptopoulou, C.P.; Perlepes, S.P.; Manessi-Zoupa, E.; Kostakis, G.E. One-dimensional cadmium(II)/bicinate(-1) complexes: The role of the alkali metal ion used in the reaction medium. *Polyhedron* **2011**, *30*, 397–404. [[CrossRef](#)]
16. Katsoulakou, E.; Konidaris, K.F.; Raptopoulou, C.P.; Psycharis, V.; Manessi-Zoupa, E.; Perlepes, S.P. Synthesis, X-ray structure, and characterization of *Catena*-bis(benzoate)bis(*N,N*-bis(2-hydroxyethyl)glycinate)cadmium(II). *Bioinorg. Chem. Applic.* **2010**, 281932.
17. Katsoulakou, E.; Bekiari, V.; Raptopoulou, C.P.; Terzis, A.; Manessi-Zoupa, E.; Powell, A.; Perlepes, S.P. Simultaneous coordination of a ketone by two cadmium(II) ions and conversion to its *gem*-diolate(-1) form. *Inorg. Chem. Commun.* **2011**, *14*, 1057–1060. [[CrossRef](#)]
18. Stamatatos, T.C.; Katsoulakou, E.; Nastopoulos, V.; Raptopoulou, C.P.; Manessi-Zoupa, E.; Perlepes, S.P. Cadmium carboxylate chemistry: Preparation, crystal structure, and thermal and spectroscopic characterization of the one-dimensional polymer  $[Cd(O_2CMe)(O_2CPh)(H_2O)_2]_n$ . *Z. Nat. B* **2003**, *58*, 1045–1054. [[CrossRef](#)]
19. Papatriantafyllopoulou, C.; Raptopoulou, C.P.; Terzis, A.; Janssens, J.F.; Manessi-Zoupa, E.; Perlepes, S.P.; Plakatouras, J.C. Assembly of a helical zinc(II) chain and a two-dimensional cadmium(II) coordination polymer using picolinate and sulfate anions as bridging ligands. *Polyhedron* **2007**, *26*, 4053–4064. [[CrossRef](#)]
20. Papatriantafyllopoulou, C.; Kostakis, G.E.; Raptopoulou, C.P.; Terzis, A.; Perlepes, S.P.; Plakatouras, J.C. Investigation of the  $MSO_4 \cdot xH_2O$  ( $M = Zn, x = 7; M = Cd, x = 8/3$ )/methyl 2-pyridyl ketone oxime reaction system: A novel Cd(II) coordination polymer versus mononuclear and dinuclear Zn(II) complexes. *Inorg. Chim. Acta* **2009**, *362*, 2361–2370. [[CrossRef](#)]
21. Milios, C.J.; Stamatatos, T.C.; Perlepes, S.P. The coordination chemistry of pyridyl oximes. *Polyhedron* **2006**, *25*, 134–194. [[CrossRef](#)]
22. Danelli, P.; Lada, Z.G.; Raptopoulou, C.P.; Psycharis, V.; Stamatatos, T.C.; Perlepes, S.P. Doubly thiocyanato(S,N)-bridged dinuclear complexes of mercury from the use of 2-pyridyl oximes as capping ligands. *Curr. Inorg. Chem.* **2015**, *5*, 26–37. [[CrossRef](#)]
23. Konidaris, K.F.; Polyzou, C.D.; Kostakis, G.E.; Tasiopoulos, A.J.; Roubeau, O.; Teat, S.J.; Manessi-Zoupa, E.; Powell, A.K.; Perlepes, S.P. Metal ion-assisted transformations of 2-pyridinealdoxime and hexafluorophosphate. *Dalton Trans.* **2012**, *41*, 2862–2865. [[CrossRef](#)]
24. Tsantis, S.T.; Zagoraiou, E.; Savvidou, A.; Raptopoulou, C.P.; Psycharis, V.; Holynska, M.; Perlepes, S.P. Binding of oxime group to uranyl ion. *Dalton Trans.* **2016**, *45*, 9307–9319. [[CrossRef](#)] [[PubMed](#)]
25. Anastasiadis, N.C.; Polyzou, C.D.; Kostakis, G.E.; Bekiari, V.; Lan, Y.; Perlepes, S.P.; Konidaris, K.F.; Powell, A.K. Dinuclear lanthanide(III)/zinc(II) complexes with methyl 2-pyridyl ketone oxime. *Dalton Trans.* **2015**, *44*, 19791–19795. [[CrossRef](#)] [[PubMed](#)]
26. Polyzou, C.D.; Lada, Z.G.; Terzis, A.; Raptopoulou, C.P.; Psycharis, V.; Perlepes, S.P. The *fac* diastereoisomer of tris(2-pyridinealdoximate)cobalt(III) and a cationic cobalt(III) complex containing both the neutral and anionic forms of the ligand: Synthetic, structural and spectroscopic studies. *Polyhedron* **2014**, *79*, 29–36. [[CrossRef](#)]
27. Stamatatos, T.C.; Papatriantafyllopoulou, C.; Katsoulakou, E.; Raptopoulou, C.P.; Perlepes, S.P. 2-pyridyloximate clusters of cobalt and nickel. *Polyhedron* **2007**, *26*, 1830–1834. [[CrossRef](#)]
28. Nikolaou, H.; Terzis, A.; Raptopoulou, C.P.; Psycharis, V.; Bekiari, V.; Perlepes, S.P. Unique dinuclear, tetrakis(nitrato-*O,O'*)-bridged lanthanide(III) complexes from the use of pyridine-2-amidoxime: Synthesis, structural studies and spectroscopic characterization. *J. Surf. Interfaces Mat.* **2014**, *2*, 311–318. [[CrossRef](#)]
29. Papatriantafyllopoulou, C.; Stamatatos, T.C.; Wernsdorfer, W.; Teat, S.J.; Tasiopoulos, A.J.; Escuer, A.; Perlepes, S.P. Combining azide, carboxylate and 2-pyridyloximate ligands in transition-metal chemistry: Ferromagnetic  $Ni^{II}_5$  clusters with a bowtie skeleton. *Inorg. Chem.* **2010**, *49*, 10486–10496. [[CrossRef](#)] [[PubMed](#)]
30. Polyzou, C.D.; Koumoussi, E.S.; Lada, Z.G.; Raptopoulou, C.P.; Psycharis, V.; Rouzières, M.; Tsipis, A.C.; Mathioniere, C.; Clérac, R.; Perlepes, S.P. “Switching on” the single-molecule magnet properties within a series



- of dinuclear cobalt(III)-dysprosium(III) 2-pyridyloximate complexes. *Dalton Trans.* **2017**, *46*, 14812–14825. [[CrossRef](#)]
31. Polyzou, C.D.; Nikolaou, H.; Papatriantafyllopoulou, C.; Psycharis, V.; Terzis, A.; Raptopoulou, C.P.; Escuer, A.; Perlepes, S.P. Employment of methyl 2-pyridyl ketone oxime in 3d/4f-metal chemistry: Dinuclear nickel(II)/lanthanide(III) species and complexes containing the metals in separate ions. *Dalton Trans.* **2012**, *41*, 13755–13764. [[CrossRef](#)]
  32. Stoumpos, C.C.; Inglis, R.; Roubeau, O.; Sartzi, H.; Kitos, A.A.; Milios, C.J.; Aromi, G.; Tasiopoulos, A.J.; Nastopoulos, V.; Brechin, E.K.; et al. Rare oxidation-state combinations and unusual structural motifs in hexanuclear Mn complexes using 2-pyridyloximate ligands. *Inorg. Chem.* **2010**, *49*, 4388–4390. [[CrossRef](#)]
  33. Stamatatos, T.C.; Foguet-Albiol, D.; Lee, S.-C.; Stoumpos, C.C.; Raptopoulou, C.P.; Terzis, A.; Wernsdorfer, W.; Hill, S.O.; Perlepes, S.P.; Christou, G. “Switching on” the properties of single-molecule magnetism in triangular manganese(III) complexes. *J. Am. Chem. Soc.* **2007**, *129*, 9484–9499. [[CrossRef](#)]
  34. Coxall, R.A.; Harris, S.G.; Henderson, D.K.; Parsons, S.; Tasker, P.A.; Winpenny, R.E.P. Inter-ligand reactions: In situ formation of new polydentate ligands. *J. Chem. Soc. Dalton Trans.* **2000**, 2349–2356. [[CrossRef](#)]
  35. Taga, T.; Uchiyama, A.; Machida, K.; Miyasaka, T. Structure of (*E*)-phenyl 2-pyridyl ketone oxime. *Acta Cryst. C* **1990**, *46*, 2241–2243. [[CrossRef](#)]
  36. Rodriguez-Mora, M.I.; Reyes-Martinez, R.; Flores-Alamo, M.; Garcia, J.J.; Morales-Morales, D. A second monoclinic polymorph of (*E*)-phenyl(pyridin-2-yl)methanone oxime. *Acta Cryst. E* **2013**, *69*, o310. [[CrossRef](#)]
  37. Ivanova, B.; Spitteller, M. A novel UV-MALDI-MS analytical approach for determination of halogenated phenyl-containing pesticides. *Ecotoxicol. Env. Saf.* **2013**, *91*, 86–95. [[CrossRef](#)]
  38. Yang, H. Trichloridotris(*N*-[phenyl(pyridin-2-yl)methylidene]hydroxylamine- $\kappa^2N,N'$ )neodymium(III). *Acta Cryst. E* **2012**, *68*, m578–m579. [[CrossRef](#)] [[PubMed](#)]
  39. Lei, T.; Chen, W.; Chen, Y.; Hu, B.; Li, Y. Trichloridotris(*N*-[phenyl(pyridin-2-yl)methylidene]hydroxylamine- $\kappa^2N,N'$ )samarium(III). *Acta Cryst. E* **2012**, *68*, m344–m345. [[CrossRef](#)] [[PubMed](#)]
  40. Holynska, M. Formation of Ni(II) oxime-bridged basket-like complexes and their structural aspects. *Curr. Inorg. Chem.* **2015**, *5*, 64–70. [[CrossRef](#)]
  41. Holynska, M. Iridium(III) products isolated in a reaction of IrCl<sub>3</sub> with phenyl 2-pyridyl ketoxime. *Zeitschrift für Kristallographie* **2013**, *228*, 72–76. [[CrossRef](#)]
  42. Yin, J.-Z.; Liu, G.-X. Dichloridobis(phenyl 2-pyridyl ketone oxime)nickel(II) acetone solvate. *Acta Cryst. E* **2009**, *65*, m155. [[CrossRef](#)]
  43. Holynska, M. Mononuclear manganese(II) complexes of phenyl 2-pyridyl ketoxime-models for studies of Q-band EPR properties. *Zeitschrift für Kristallographie* **2012**, *227*, 831–836. [[CrossRef](#)]
  44. Martinez, J.; Aiello, I.; Bellusci, A.; Crispini, A.; Ghedini, M. Tetranuclear zinc complexes of ligands containing the 2-pyridyl oxime chelating site. *Inorg. Chim. Acta* **2008**, *361*, 2677–2682. [[CrossRef](#)]
  45. Wong, J.S.-Y.; Wong, W.-T. Synthesis, structural characterization and reactivity of triosmium carbonyl clusters containing oxime ligands. *New J. Chem.* **2002**, *26*, 94–104. [[CrossRef](#)]
  46. Yan, J.; Liu, G.-X. Tris(phenyl 2-pyridyl ketone oxime- $\kappa^2N,N'$ )cadmium(II) dinitrate. *Acta Cryst. E* **2009**, *65*, m641. [[CrossRef](#)] [[PubMed](#)]
  47. Tangoulis, V.; Raptopoulou, C.P.; Terzis, A.; Paschalidou, S.; Perlepes, S.P.; Bakalbassis, E.G. Octanuclearity in copper(II) chemistry: Preparation, characterization, and magnetochemistry of [Cu<sub>8</sub>(dpk-OH)<sub>8</sub>(O<sub>2</sub>CCH<sub>3</sub>)<sub>4</sub>](ClO<sub>4</sub>)<sub>4</sub>·9H<sub>2</sub>O (dpk-H<sub>2</sub>O= the hydrated, *gem*-diol form of di-2-pyridyl ketone). *Inorg. Chem.* **1997**, *36*, 3996–4006. [[CrossRef](#)]
  48. Papatriantafyllopoulou, C.; Efthymiou, C.G.; Raptopoulou, C.P.; Terzis, A.; Manessi-Zoupa, E.; Perlepes, S.P. Mononuclear versus dinuclear complex formation in nickel(II) sulfate/phenyl(2-pyridyl) ketone oxime chemistry depending on the ligand to metal reaction ratio: Synthetic, spectral and structural studies. *Spectrochim. Acta A* **2008**, *70*, 718–728. [[CrossRef](#)]
  49. Egidike, I.P. Cu(II) complexes of 4-[(1*E*)-*N*-(2-[(*Z*)-benzylidene-amino]ethyl)ethanimidoyl]benzene-1,3-diol Schiff base: Synthesis, spectroscopic, in-vitro antioxidant, antifungal and antibacterial studies. *Molecules* **2018**, *23*, 1581. [[CrossRef](#)]
  50. Dollish, F.R.; Fateley, W.G.; Bentley, F.F. *Characteristic Raman Frequencies of Organic Compounds*; John Wiley and Sons: New York, NY, USA, 1974; pp. 135–137, 162–190, 263–272.
  51. Lopez-Garriga, J.J.; Babcock, G.T.; Harrison, J.F. Factors influencing the C=N stretching frequency in neutral and protonated Schiff's bases. *J. Am. Chem. Soc.* **1986**, *108*, 7241–7251. [[CrossRef](#)]

52. Dullien, F. Raman spectra and configuration of some  $\alpha$ -furyl and  $\alpha$ -benzofuryl ketoximes. *Can. J. Chem.* **1957**, *35*, 1366–1374. [[CrossRef](#)]
53. Suvitha, A.; Periandy, S.; Boomadevi, S.; Govindarajan, M. Vibrational frequency analysis, FT-IR, FT-Raman, ab initio, HF and DFT studies, NBO, HOMO-LUMO and electronic structure calculations on pycolinaldehyde oxime. *Spectrochim. Acta A* **2014**, *117*, 216–224. [[CrossRef](#)]
54. Adams, D.M. *Metal-Ligand and Related Vibrations: A Critical Survey of the Infrared and Raman Spectra of Metallic and Organometallic Compounds*; Edward Arnold Publishers: London, UK, 1967; pp. 45, 79.
55. Dilella, D.P.; Stidham, H.D. Vibrational Spectra of C<sub>2v</sub> Deuterium Substituted Pyridines. *J. Raman Spectrosc.* **1980**, *9*, 90–106. [[CrossRef](#)]
56. Muniz-Miranda, M. On the occurrence of the central line ( $\sim 1025\text{ cm}^{-1}$ ) in the SERS spectra of pyridine absorbed on silver hydrosols. *Chem. Phys. Lett.* **2001**, *340*, 437–443. [[CrossRef](#)]
57. Andrade, G.F.S.; Temperini, M.L.A. Identification of species formed after pyridine adsorption on iron, cobalt, nickel and silver electrodes by SERS and theoretical calculations. *J. Raman Spectrosc.* **2009**, *40*, 1989–1995. [[CrossRef](#)]
58. Zaitsev, A.B.; Vasil'tsov, A.M.; Schmidt, E.Y.; Mikhaleva, A.I.; Morozova, L.V.; Afonin, A.V.; Ushakov, I.A.; Trofimov, B.A. O-vinyldiaryl- and O-vinylaryl(hetaryl) ketoximes: A breakthrough in O-vinyloxime chemistry. *Tetrahedron* **2002**, *58*, 10043–10046. [[CrossRef](#)]
59. Jackman, L.M.; Sternhell, S. *Applications of Nuclear Magnetic Resonance Spectroscopy in Organic Chemistry*, 2nd ed.; Pergamon Press: Oxford, UK, 1969; pp. 216, 226.
60. Geary, W.J. The use of conductivity measurements in organic solvents for the characterization of coordination compounds. *Coord. Chem. Rev.* **1971**, *7*, 81–122. [[CrossRef](#)]
61. *CrystalClear*; Rigaku: The Woodlands, TX, USA; MSC Inc.: The Woodlands, TX, USA, 2005.
62. Sheldrick, G.M. A short history of SHELX. *Acta Cryst. A* **2008**, *64*, 112–122. [[CrossRef](#)]
63. Sheldrick, G.M. Crystal structure refinement with SHELXL. *Acta Cryst. C* **2015**, *71*, 3–8. [[CrossRef](#)] [[PubMed](#)]
64. *Diamond, Crystal and Molecular Structure Visualization, Ver. 3.1*; Crystal Impact: Bonn, Germany, 2018.

**Sample Availability:** Samples of the compounds **1**·H<sub>2</sub>O and **2** are available from the authors.



© 2019 by the authors. Licensee MDPI, Basel, Switzerland. This article is an open access article distributed under the terms and conditions of the Creative Commons Attribution (CC BY) license (<http://creativecommons.org/licenses/by/4.0/>).